E3S Web of Conferences **709**, 06005 (2026) https://doi.org/10.1051/e3sconf/202670906005
ICERE 2026

CFD Assessment of Age-of-Air Distribution and Air-Change Effectiveness in a Detention Facility

John Nico Omlang[1*], and *Jerome* Lopena[1]

[1]Mechanical Engineering Department, FEU Institute of Technology, Sampaloc, Manila, 1015, Philippines

Abstract. Overcrowded detention cells often suffer from inadequate ventilation, posing significant health risks to inmates due to the buildup of airborne contaminants. To improve indoor air quality and comfort in such confined environments, this study investigates the influence of different supply air configurations on the age-of-air (AoA) distribution and air-change effectiveness (ACE) in detention cells of a city jail in the Philippines. Computational Fluid Dynamics (CFD) simulations using the standard k–ε turbulence model with scalable wall functions were conducted to evaluate four ventilation setups varying in the number of ducting lines and air supply grilles. CFD serves as a powerful and non-intrusive tool for analyzing ventilation systems, particularly in environments where physical testing is impractical or unsafe. Results show that configurations with three ducting lines provide more uniform airflow distribution across bunk levels, while increasing the number of supply air grilles decreases the average AoA and enhances ACE. Among the four setups, the configuration with three ducting lines and ten supply air grilles per duct achieved the most balanced performance in terms of airflow comfort and ventilation efficiency. The findings highlight the potential of CFD-assisted design optimization in improving air quality management in detention facilities and other densely occupied confined spaces.

1 Introduction

Detention and prison facilities are crucial components of any judicial system, playing a significant role in maintaining societal law and order. However, the living conditions for detainees or inmates are of utmost importance. Challenges faced by inmates, such as overcrowding and inadequate ventilation, can lead to severe health issues [1-3]. Overcrowding and poor ventilation in prison facilities also increase the risk of infectious disease transmission [4-5]. Additionally, inadequate air exchange between indoor and outdoor spaces can result in poor air quality, further affecting health [6]. Ensuring sufficient air circulation, especially in confined areas like detention cells, is crucial for improving occupants' well-being.

Computational Fluid Dynamics (CFD) simulation software is a valuable tool for evaluating ventilation system performance, aiding designers and researchers in finding

* Corresponding author: jnomlang@feutech.edu.ph

suitable configurations. It was selected as the primary analysis tool because it provides a non-intrusive, cost-effective, and highly detailed method for assessing ventilation performance in complex or inaccessible environments. Unlike experimental approaches, which are often limited by measurement constraints and safety concerns in detention facilities, CFD allows the visualization and quantification of airflow patterns under controlled boundary conditions. This capability enables researchers and designers to evaluate and optimize ventilation system performance before implementation, ensuring improved air distribution efficiency and occupant comfort. Important parameters to consider in CFD analysis include air velocity, age-of-air (AoA), and air-change effectiveness (ACE) [7-8]. AoA measures the time fresh air takes to reach a specific point, while ACE gauges the system's efficiency in removing air contaminants.

Previous studies have analyzed AoA distribution in various ventilation scenarios in classrooms [9], hospital wards [10], and naturally ventilated buildings [7]. While previous studies explored AoA and ACE in various facilities, limited attention has been given to correctional environments, where ventilation design directly affects infection transmission risk. As for this research study, the focus is to determine the influence of ventilation setup in the AoA distribution and ACE and identify the optimal configuration among the four scenarios of ventilation systems proposed for detention cells in a city jail in the Philippines. The configurations were evaluated in terms of AoA and ACE using CFD analysis. This study is significant since it can be used as a basis in designing or retrofitting ventilation systems in detention facilities.

2 Methodology

2.1 Design Configurations

The design configurations considered are presented in Table 1 with variation in number of ducting lines and the number of supply air grilles. The ventilation system for all the configurations uses a 3840 CFM supply air fan with 2 inches water static pressure and 3840 CFM exhaust fan.

Table 1. Design configurations of the ventilation system design.

Configuration	Number of ducting lines	Number of supply air grilles per duct
Configuration 1	3	4
Configuration 2	3	10
Configuration 3	2	4
Configuration 4	2	10

2.2 Design Parameters

This section presents the design parameters used to evaluate the effectiveness of each configuration.

2.2.1 Velocity

The velocity of the wind is one of the factors to consider in addressing the comfort condition of the domain of each cell. The Lawson comfort criteria provide a standard for wind comfort for a wide range of activities. The applicability of this standard transcends outdoor scenarios and extends to the evaluation of indoor environments. Since detainees often spend a substantial portion of their time sitting on bunk beds, the suitable activity is the "sitting long" condition. The comfortable wind velocity for this scenario ranges from 0 to 2.5 m/s based on the general Lawson wind comfort criteria [11].

2.2.2 Age-of-Air (AoA)

It refers to the average amount of time that a parcel of air has spent in a particular region of space. The AoA is a crucial parameter in understanding the transport and mixing of pollutants, as well as the dispersion of gases and particles in the atmosphere. The average AoA in a system with perfect mixing is unaffected by the recirculation portion [12]. The AoA can influence how quickly potentially contaminated air is replaced with fresh outdoor air so a shorter period of AoA is desired.

2.2.3 Air Change Effectiveness (ACE)

An efficient ventilation system is one that quickly changes the air in the room while using the least amount of energy, that is, by moving as little air as possible. ACE is the ability of an air distribution system to deliver ventilation air to a building, zone, or space. The AoA is related to ACE and gives a quantitative criterion to consider in evaluating ventilation. The ratio of a nominal time constant to the mean AoA is one common definition of ACE. The nominal time constant t_n is calculated as the ratio of the domain volume (ft^3) to the domain supply air volume ($ft^3 \cdot s^{-1}$), as shown in Equation (1). The ACE can be calculated using Equation (2), where t_{AoA} is the average AoA. An ACE value less than one indicates that the zone's air distribution is less than perfect mixing. When the air-supply diffusers and return grilles don't distribute air properly, it makes the air older and reduces the ACE. The ACE will be greater than unity if air is supplied preferentially to the breathing zone [13]. In this study, the supply and exhaust fan flow rates (3840 CFM) and rated static pressure (2 in. w.g.) were kept constants for all configurations. Under this constraint, ACE can be interpreted as an indicator of ventilation energy efficiency, since a higher ACE corresponds to more effective contaminant removal for the same fan power input.

$$t_n = \frac{V_{domain}}{Q_{supply}} \quad (1)$$

$$ACE = \frac{t_n}{2 \times t_{AoA}} \quad (2)$$

2.3 Simulation Setup

The program used to perform the CFD simulation is Ansys 2019 R2, specifically the CFX in Workbench. The standard k-ε turbulence model is used to represent the flow of air inside the cells with scalable wall functions. This model was chosen because its prevalence in industrial flow and heat transfer simulations can be attributed to its robustness, efficiency, and reasonable accuracy over a wide spectrum of turbulent flows [14]. The model was analyzed under steady state condition and energy equations were neglected for all cases since the continuous supply of fresh air inside the cells will result in thermal equilibrium, that is, the properties of supplied air will be the same as the air inside the cells. The study focuses mainly on the time the air inside the domain is being replaced and how effective the air change is. A scalar volumetric type of variable was deployed with a unit of second to measure the age-of-air distribution. To ensure the validity of the results, the numerical simulation undergone grid independence analysis and showed that the results have negligible difference under varying mesh sizes from 0.025 m to 0.1 m. Hence, the use of 0.1 m mesh size was chosen to minimize the computational time.

The geometry of the domain used in the simulation is shown in Figure 1. The supply air grilles dimension a×b and the distance between the supply grilles c vary in each configuration. For configurations 1 and 3, the dimension a×b is 10 inches by 8 inches and c is 2100 millimeters, while for configurations 2 and 4, a×b is 6 inches by 6 inches and c is 700 millimeters. For all the configurations, the exhaust grille dimension is 36 inches by 24 inches.

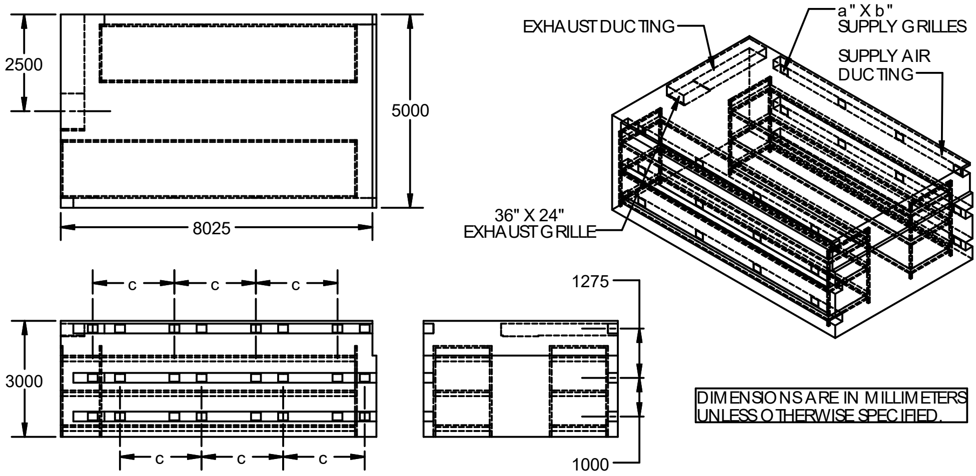

Fig. 1. Geometry details of the domain for CFD simulation

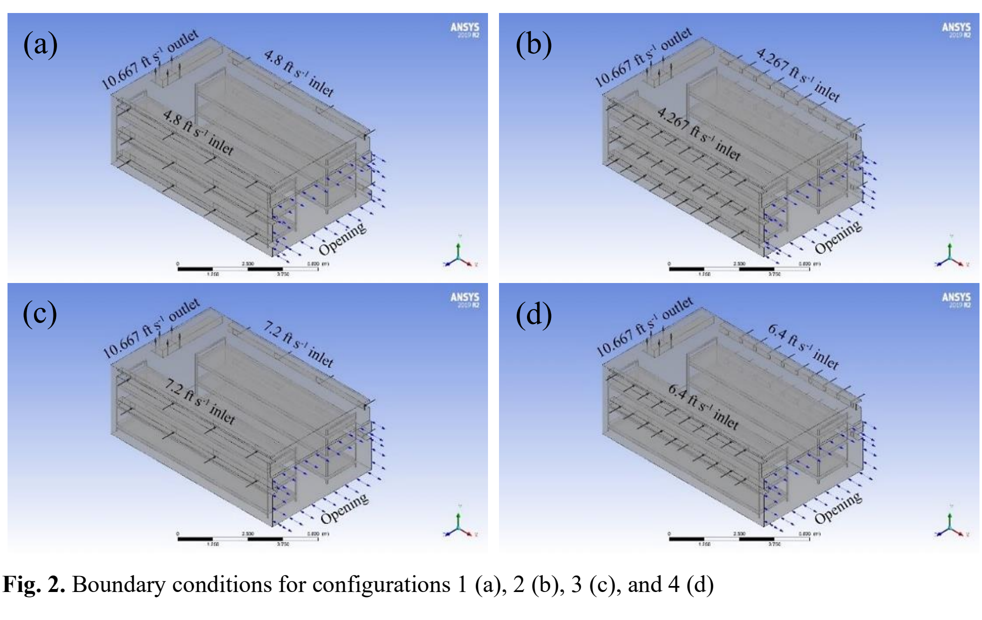

Fig. 2. Boundary conditions for configurations 1 (a), 2 (b), 3 (c), and 4 (d)

The boundary conditions for each configuration are presented in Figure 2. The black arrows directed toward the domain are the inlet boundary condition that represents the supply air from the grilles while those directed outside the domain are outlet boundary condition which represent the exhaust grilles. The blue arrows show the opening boundary condition and that is where the rails are located.

2.4 Validation of CFD Model

The accuracy and reliability of the CFD model developed in this study were verified through comparison with benchmark results obtained from a previous study that investigated ventilation efficiency in a controlled test chamber using the age-of-air (AoA) concept [16]. In the referenced study, the researchers computed the Local Mean Age (LMA) and Local Mean Residual Lifetime (LMR) through a user-defined function (UDF) embedded in ANSYS Fluent, which enabled the simulation of tracer-gas transport and the prediction of air exchange dynamics within the chamber. The numerical results were then validated experimentally using a tracer-gas decay method to ensure the physical accuracy of the model. Their findings showed strong agreement between the CFD and experimental results, with reported correlation coefficients ranging from 0.91 to 0.96. This high level of correlation confirmed that the CFD model was capable of accurately capturing airflow behavior, contaminant transport, and ventilation performance under the defined boundary and operating conditions. By aligning the present model validation process with this established benchmark, confidence in the predictive capability of the developed CFD model was ensured.

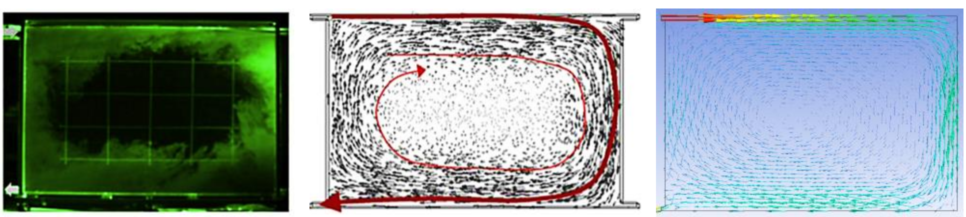

Fig. 3. Visualization of Experimental Result (Kwon et al., 2011) (leftmost), CFD Result (Kwon et al., 2011) (middle), and CFD Result of the Present Study (rightmost).

To ensure that the present CFD model produces physically realistic and reliable results, model validation was carried out by replicating the flow conditions of Case 3-3 from the benchmark experimental and numerical study [15]. A qualitative comparison of the airflow structure between the benchmark experimental visualization, the reference CFD results, and the present simulation is presented in Figure 3, highlighting the consistency of the dominant recirculation pattern and global flow behavior. This particular case represents a fully developed airflow regime corresponding to an air exchange rate (AER) of 2.0, which provides an appropriate basis for evaluating the accuracy of the simulated ventilation performance. The same numerical setup was adopted in the present work, including the use of the standard k–ε turbulence model, the finite-volume discretization scheme, and identical boundary conditions, to ensure direct comparability and methodological consistency with the validated reference. The validation procedure involved a detailed comparison of airflow velocity and age-of-air (AoA) values at corresponding measurement points defined in the reference study. This approach allowed for a quantitative assessment of the model's ability to reproduce the established flow characteristics and temporal air distribution patterns under controlled ventilation conditions.

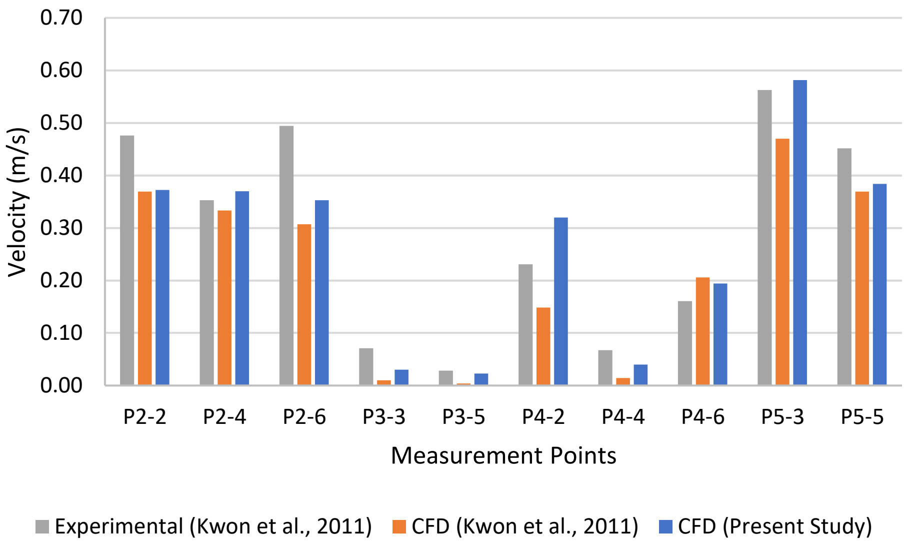

Fig. 4. Comparison of air velocity between present study and Kwon et al. (2011).

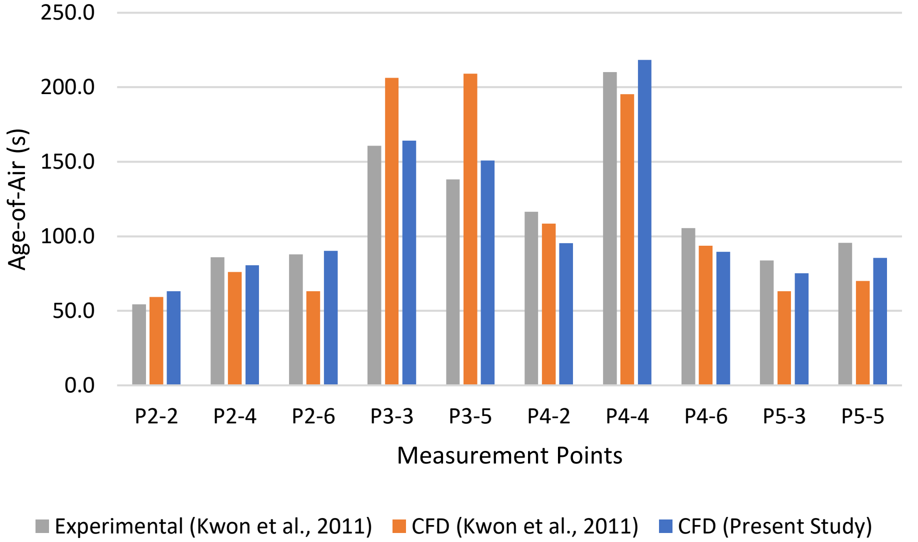

Fig. 5. Comparison of average age-of-air between present study and Kwon et al. (2011).

Figures 4 and 5 present the comparison of air velocity and average age-of-air (AoA) between the present study and the previous study, respectively. The predicted velocity profile followed the same spatial trend as the reference data, with higher velocities near the air inlet and decreasing magnitudes toward the center region. The computed Pearson correlation coefficient (r) between the two datasets was 0.9405, indicating an excellent level of agreement. Similarly, the comparison of AoA values showed consistent patterns, with lower values near the air supply region and higher values within recirculation zones. The resulting correlation coefficient of 0.9757 demonstrates very strong consistency between the predicted AoA values and those reported in the validated benchmark case.

These high correlation coefficients confirm that the present CFD model accurately reproduces the airflow dynamics and ventilation characteristics observed in the validated experimental and numerical data of the previous study. The close agreement in both velocity and AoA distributions verifies that the current numerical setup is capable of reliably predicting airflow behavior, mixing efficiency, and air renewal within confined environments. Consequently, the present CFD model is considered both numerically and statistically validated, providing a robust foundation for the subsequent analysis of air-change effectiveness (ACE) and ventilation performance in detention cell configurations.

3 Results and Discussion

Figure 6 displays velocity gradients for the four configurations. Configuration 2, with 60 total supply air grilles, exhibits the most favorable velocity distribution. Both configurations 1 and 2, with three ducting lines, provide superior velocity distribution across bunk levels compared to configurations 3 and 4, which only have two ducting lines. Configurations with two ducting lines, where one is on the wall side of the top bunk and the other on the middle bunk, show slightly less velocity distribution in the bottom bunk level. Average velocities for configurations 1 to 4 are 0.83 ft/s, 0.72 ft/s, 0.90 ft/s, and 0.89 ft/s, respectively, as shown in Table 2. Configurations with two ducting lines achieve higher average velocities, possibly due to concentrated air distribution in the top and middle bunk levels. Nevertheless, all average velocities fall within the comfortable wind speed range (0 to 8.2 ft/s) based on the general Lawson wind comfort criteria [11].

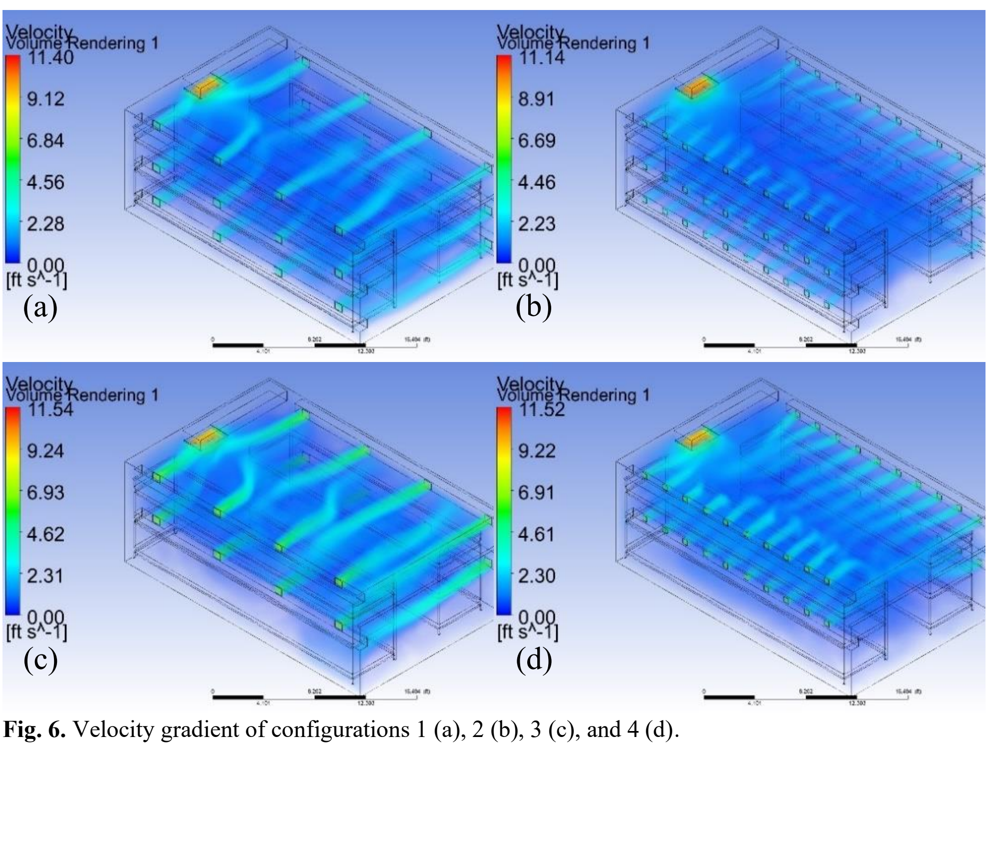

Fig. 6. Velocity gradient of configurations 1 (a), 2 (b), 3 (c), and 4 (d).

 https://doi.org/10.1051/e3sconf/202670906005

Table 2. Summary of results for each configuration.

Configuration	Average velocity (ft s^{-1})	Average AoA (s)	t_n (s)	ACE
1	0.83	42.93	63.03	73.40%
2	0.72	39.97	63.03	78.84%
3	0.90	46.57	63.56	68.24%
4	0.89	41.03	63.56	77.45%

Figure 7 illustrates the AoA distribution for the four configurations. Average AoA values for configurations 1 to 4 are 42.93 s, 39.97 s, 46.57 s, and 41.03 s, respectively, as presented in Table 2. Configuration 2 boasts the lowest average AoA, signifying improved air movement as evident in figure 4(b) due to its higher number of supply air grilles (60 pcs). The lower AoA values in configuration 2 indicate faster air renewal, which implies reduced accumulation of contaminants such as CO_2 and aerosols which are critical for infection control in detention environments. Configuration 4, with 40 supply air grilles, achieved the second lowest average AoA but suffered from higher AoA at the bottom bunk level as a result of its 2-line ducting setup as shown in figure 4(d). Configuration 3, with the least number of air supply grilles (16 pcs), had the highest average AoA, along with high AoA at the lower bunk level as shown in figure 4(c) caused by its 2-line ducting configuration.

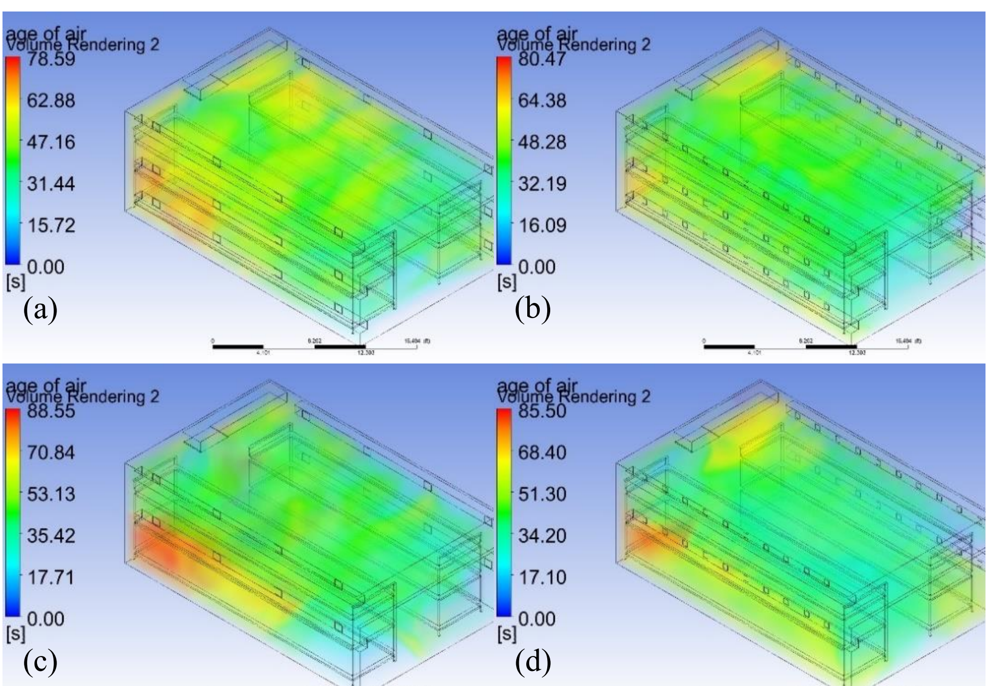

Fig. 7. Age-of-air distribution of configurations 1 (a), 2 (b), 3 (c), and 4 (d).

4 Conclusion

In this study, the air velocity distribution, average AoA and ACE of four configurations of ventilation systems for detention cells in a city jail were analyzed through CFD simulations. In general, better air distribution in each level of bunk bed of the detention cell is observed in the configurations with three-line ducting. On the other hand, the configurations with higher number of supply air grilles achieved lower values of AoA that resulted to higher ACE. Among the scenarios, configuration 2 that has a three-line ducting and 10 supply air grilles per duct is the best option. It achieved the shortest average AoA (39.97 s) and the highest ACE (78.84 %). Alternatively, configuration 4 can be an option depending on the difference in cost when compared to configuration 2. This will lessen the cost since it only has 2 lines of ducting, but the ACE (77.45 %) is not that far from configuration 2 and it also has the 2nd lowest AoA (41.03 s).

The findings in this study suggest that retrofitting of existing detention cells should prioritize airflow uniformity and contaminant removal through AoA analysis without excessive mechanical complexity. Future work may include transient or contaminant transport analysis to further assess ventilation performance under dynamic conditions.

References

1. J.N. Eze, O.B. Ozoh, F.C. Otuu, E.N. Shu, B.U. Anyaehie, BMC Pulm. Med. **22**, 84 (2022)
2. F. Otuu, C. Okwuosa, I. Maduka, S. Ogbodo, I. Shuneba, H. Nkechi, E.N. Shu, Adv. Clin. Toxicol. **4**, 1 (2019)
3. J. Urrego, A.I. Ko, A.S.S. Carbone, D.S.G. Paião, R.V.E. Sgarbi, C.W. Yeckel, J.R. Andrews, J. Croda, Am. J. Trop. Med. Hyg. **93**, 739 (2015)
4. J. Wang, W. Yang, L. Pan, J.S. Ji, J. Shen, K. Zhao, B. Ying et al., Environ. Pollut. **266**, 115161 (2020)
5. H.B. Mera, F. Wagnew, Y. Akelew, Z. Hibstu, S. Berihun, W. Tamir, S. Alemu et al., Tuberc. Res. Treat. **2023**, 6226200 (2023)
6. X. Sui, Z. Tian, H. Liu, H. Chen, D. Wang, J. Build. Eng. **42**, 103040 (2021)
7. C. Buratti, D. Palladino, Appl. Sci. **10**, 1730 (2020)
8. V. Adjiski, D. Mirakovski, Z. Despodov, S. Mijalkovski, Min. Sci. **25**, 175 (2018)
9. S.-H. Park, K.-R. Lee, S.-J. Yook, H.B. Koo, Toxics **10**, 545 (2022)
10. J.-H. Noh, J. Lee, K.-C. Noh, Y.-W. Kim, S.-J. Yook, Aerosol Air Qual. Res. **18**, 2643 (2018)
11. T.V. Lawson, J. Wind Eng. Ind. Aerodyn. **3**, 93 (1978)
12. C.C. Federspiel, Indoor Air **9**, 47 (1999)
13. K. Gungor, Ecolibrium **12**, 32 (2013)
14. ANSYS Inc., ANSYS Fluent Theory Guide **15**, 47 (2017)
15. K.-S. Kwon, I.-B. Lee, H.-T. Han, C.-Y. Shin, H.-S. Hwang, S.-W. Hong, J.P. Bitog, I.-H. Seo, C.-P. Han, Biosyst. Eng. **110**, 421 (2011)